16th World Conference on Earthquake, 16WCEE 2017

Santiago Chile, January 9th to 13th 2017

Paper N° 1882

Registration Code: S-V1465902705

DAMAGE CONTROLLING PERFORMANCE OF A FULL SCALE UNBONDED POST-TENSIONED PRECAST CONCRETE BEAM

T. Obara[(1)], H. Watanabe[(2)], S. Kono[(3)] and T. Okayasu[(4)]

[(1)] *Ph.D. candidate, Tokyo Institute of Technology, obara.t.ac@m.titech.ac.jp*
[(2)] *Assistant Professor, Tokyo Institute of Technology, watanabe.h.as@m.titech.ac.jp*
[(3)] *Professor, Tokyo Institute of Technology, kono.s.ae@m.titech.ac.jp*
[(4)] *Research Engineer, Technical Research Institute, Kajima Corporation, okayasu@kajima.com*

Abstract

Twenty-some years ago, it was considered that safety was a major and only concern in designing building structures in an engineering society. However, the 1994 Northridge earthquake and 1995 Kobe Earthquake revealed that the general public does not share the same vision with the engineering society. Urban earthquakes of last twenty years made the general public and the engineering society confident that structures need to perform in a higher standard, that is, damage of structures should be minimal so that structures should keep their functions after multiple earthquakes. Since then, new structural systems such as base isolation system and response controlling system with dampers have been attracting attentions. However, these systems are not necessarily universal and other variations of structural systems are also needed to meet different demand. A self-centering rocking system using unbonded post-tensioned precast concrete members is one of good alternatives for damage-controlling structures. By using high quality precast concrete, the rocking system is very durable in long term and damage-resistant in a short term. Unbonded post-tensioned precast concrete system is able to reduce cracking as well as residual deformation/displacement and maintain structural functions for its self-centering property.

In this research, a static loading test was conducted on a full-scale unbonded post-tensioned precast concrete H-shaped beam-column assemblage. The objective was to quantitatively evaluate the damage at different loading stages. The 600mm x 1000mm beam with clear span length of 11 meters was post-tensioned with four unbonded strands to column at both ends. Two columns had pin-joints at their top and bottom to simulate the intermediate story of a building. Two point loads of 230kN each were applied to the beam to simulate vertical load due to dead and live load. The experimental results showed satisfactory seismic performance with minor damage and less residual drift and the specimen conformed to requirements for continuous use of members defined in the AIJ guidelines. In addition, the residual crack width, residual deformation drift and equivalent damping ratio were evaluated using the AIJ guidelines to study the validity of the criteria. It was concluded that a full-scale unbonded post-tensioned precast concrete beam possessed good seismic performance of quick recovery and functional maintenance.

Keywords: a full scale frame, unbonded post-tensioned precast beam, damage controlling ability, hysteresis loop

1. Introduction

In the 1994 Northridge earthquake and 1995 Kobe Earthquake, even if buildings did not collapse, many buildings were not able to serve their functions due to various types of structural and nonstructural damage. The economic loss during this downtime sometimes overpass the building repair cost. In 1981, a new design law of Japan required the minimum performance level in which the building should continue in operation due to medium earthquakes and not collapse due to severe heavy earthquakes. However, the society demands have been shifting to higher levels recently. Therefore, reduction of damage of buildings and quick recovery to maintain the continuity of the building functions are very important issues. One of solutions is base isolation, but the system has high initial cost and extra space, so it cannot be applied for all kinds of buildings. Another solution is a self-centering system using unbonded prestressed precast members and energy dissipation elements. The latter system controls the damage and has less residual drift, especially with unbonded system.

The U.S. PRESSS (PREcast Seismic Structural System) project [1, 2, 3] proposed some self-centering systems. A hybrid system used unbonded tendons in beam section and mild reinforcements as energy dissipation element in the same section. This method showed excellent performances with limited or negligible seismic damage and the frame using this system had high self-centering ability. The system was already used in a 39-story building in California [4]. However, PRESSS proposed system has complex beam sections since they have prestressing tendons and energy dissipation elements at the same critical section. Therefore, Marriott et al. relocated energy dissipation elements from the critical section for a simpler system [5]. This paper introduces behaviors of a rocking system, which is the fundamental but essential part of self-centering hybrid system. The specimen was a full-scale of unbonded post-tensioned precast concrete beam with reinforced concrete columns. The paper describes the damage in terms of residual deformation angle, residual crack width and equivalent damping ratio compared with calculated values using the AIJ guidelines formula [6]. The test results were also compared with those of two half scale unbonded post-tensioned precast concrete beam specimens, PCa11 and PCa12 [7]. PCa11 and PCa12 were tested to evaluate damage levels of the cantilever beams. PCa11 and PCa12 had a cross section of 500mm x 600mm and shear span of 1800mm and 3300mm respectively. Concrete compressive strength was 70.1 N/mm^2 and axial stress level due to prestressing, η, in Eq. (1) was 0.07 for PCa11 and 0.13 for PCa12.

2. Test Program

Table 1 shows major dimensions of a full-scale unbonded post-tensioned precast concrete H-shaped beam-column assemblage (PCa20). It also shows dimensions of two half-scale of unbounded post-tensioned precast cantilever beam (previous study) as references. For PCa20, a ratio of shear capacity and flexural capacity was larger than 2.0 so that failure mode is governed by flexure. Figure 1 shows dimensions and reinforcement details. RC columns had cross section of 1000mm x 1000mm with longitudinal reinforcement of 16-D35 and transverse reinforcement of D13@100mm. Unbonded post-tensioned precast concrete beam had cross section of 600mm x 1000m with longitudinal mild reinforcement of 4－D19 and transverse reinforcement of 2－D13. Clear span length of beam was 11 meters including the thickness of joint mortar of 30mm at its both ends. Prestressing strands were inserted in corrugated sheaths with the inner diameter of 50mm. Beam and columns were cast separately and were assembled with 30mm thick joint mortar by applying prestressing force through four PS strands. A load cell was placed to measure prestressing force at the north end of each prestressing strands. Introduced prestressing force was 65% of the specified yield strength of the PS strands (η in Eq. (1) was 0.052.). The mechanical index q_{pr} in Eq. (2) was 0.044. Figure 2 and Figure 3 show mechanical properties of concrete, prestressing strands and reinforcement.

$$\eta = \frac{P_e}{b \cdot D \cdot \sigma_B} \tag{1}$$

$$q_{pr} = \frac{(T_{pc} + T_{py}) + (T_{sy} - C_{sy})}{b \cdot D \cdot \sigma_B} \tag{2}$$

P_e : initial prestressing force (N), T_{pc} : force of strands in compressive side (kN), T_{py} : force of strands in tensile side (kN), T_{sy} : yield force of tensile reinforcement (kN), C_{sy} : yield force of compressive reinforcement (kN), b : beam width (mm), D : total beam depth (mm), σ_B : concrete compressive strength (MPa).

Table 1 – Test variables

Specimen	PCa20	PCa11	PCa12
	A full scale beam	1/2 scale beam (previous research)	
Structural system	unbonded Post-tensioned Precast structure		
Concrete compressive strength	70.4N/mm^2	70.1N/mm^2	
Width x Total depth (B x D)	600mm×1000mm	500mm×600mm	
Londitudinal reinforcement	4-D19(SD345) at upper and lower position for an assemblage purpose. They are curtailed at both ends of a beam.		
Prestressing bar	4- ϕ 28.6	4- ϕ 23	4- ϕ 32
Sheath	Corrugated sheath with internal diameter of 50mm (#1050)		
Stirrups	2-D13@100 or @200(SD345)	4-D10@100 (SD295A)	
Shear span and shear span ratio (a/D)	5.5m (5.5)	1.8m (3.0)	3.3m (5.5)
Mechanical reinforcement index※ (q_{pr})	0.044	0.052	0.12
Axial stress level due to prestressing※ (η)	0.052	0.070	0.13

※The values based on the material test results.

Table 2 – Mechanical properties of concrete and joint mortar

Location	Compressive strength (MPa)	Young's modulus (GPa)	Spilitting tensile strength (MPa)
Beam	70.4	38.2	4.87
Joint mortar	62.7	26.5	3.84
Column(North)	65.7	37.1	4.60
Column(South)	67.5	37.1	4.95

Table 3 – Mechanical properties of reinforcement

	Diameter	Location	Yeild strength (MPa)	Yield strain (%)	Tensile strength (MPa)	Young's modulus (GPa)
Beam	D19	Londitudinal reinforcement	379	0.208	559	188
	D13	Transverce reinforcement	378	0.220	540	179
	ϕ 28.6	Prestressing strands※	1570	0.978	1683	202
Column	D35	Londitudinal reinforcement	457	0.247	654	199
	D13	Transverce reinforcement	378	0.220	540	179

※ Yield stress of tendons was taken as 0.2% offset yield stress. This prestressing strands consist of 19-ply.

Figure 2 shows loading system. There were two vertical jacks to simulate moment distribution of long term loading. The vertical loads were kept constant during the test. Lateral load was applied by using horizontal hydraulic jacks. Loading protocol was controlled by drift angle, R. Drift angle, R, is defined as the ratio of relative horizontal displacement between the upper and bottom clevises to the height (3.2m). The load protocol

was consisted of two cycles of R= ±0.125%, ±0.25%, ±0.5%, ±0.75%, ±1.0%, ±0.5%, ±1.5%, ±2%, ±0.5% and ±4%. Then the specimen was loaded one cycle to ±6.7%. Flexural and shear deformation of beam were measured by using displacement gauges as shown in Fig. 2 (c). The drift angle of beam R_b was calculated by using these displacement gauges.

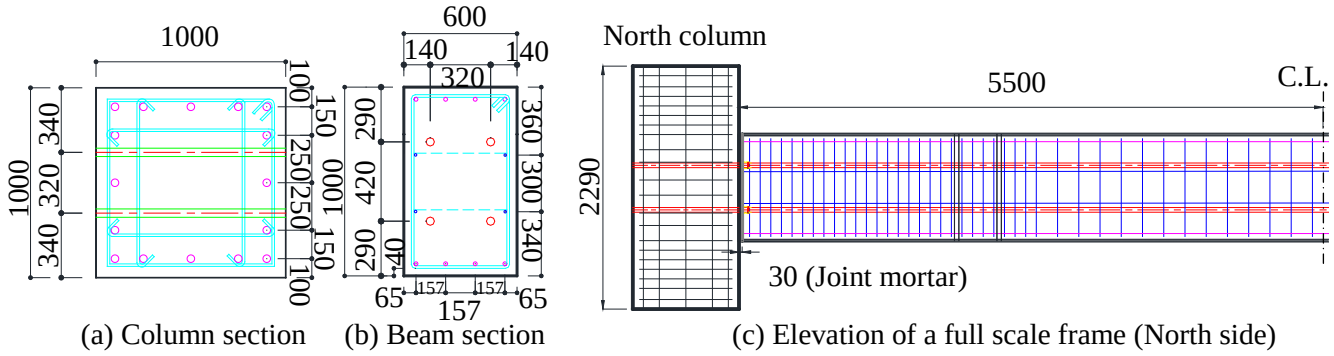

Fig. 1 – Reinforcement details and dimensions (Unit: mm)

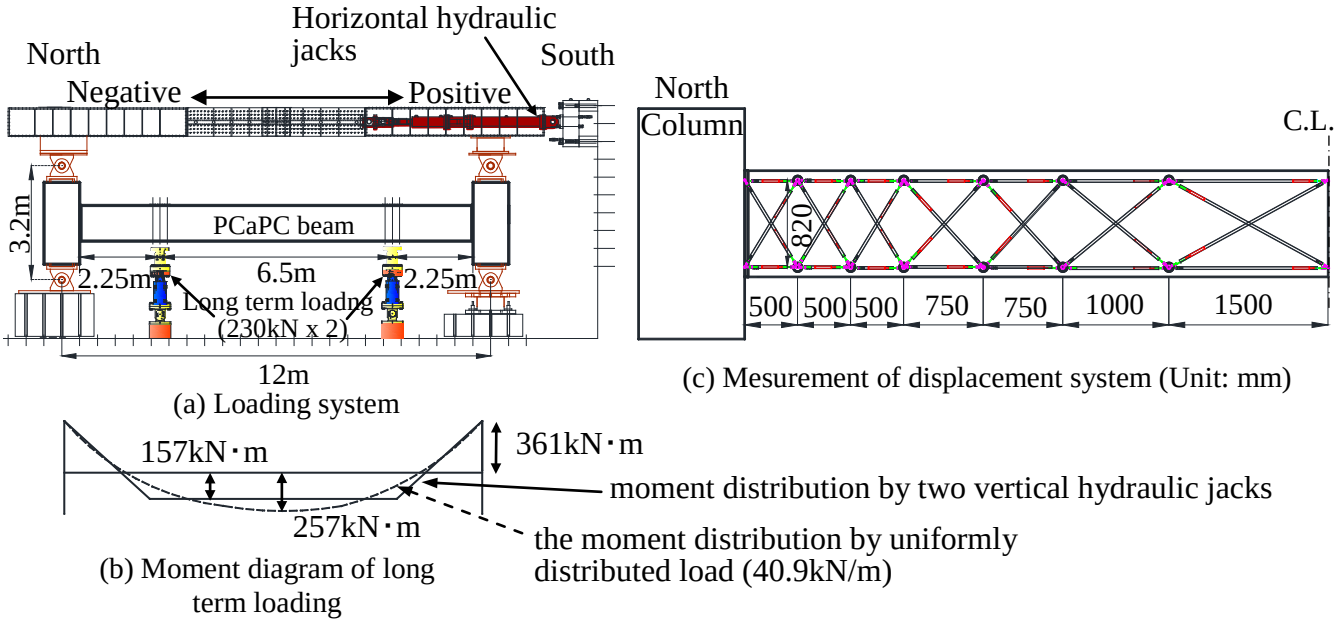

Fig. 2 – Loading and mesurement system

3. Test Results

3.1 Load (Q) – Drift angle (R) Relation

Figure 3 shows lateral load (Q) – drift angle (R) relation. The first flexural cracks appeared at the lower fiber around the vertical hydraulic jacks at *R*=±0.25% for both positive and negative loading directions. Minor compressive damage at the edge of beam occured at *R*=+1.5% and R=-1.0%. Comressive yielding of assembling reinforcement (longitudinal reinforcement) occured at *R*=+2.9% and *R*=-1.9%. The mortar at south beam column interface spalled during positive loading resulting in drop of load carrying capacity after the second cycle of R= +1.5%. Therefore, the maximum lateral load capacity was reached at R=+1.5% in the positive direction, while it was reached around R=-3.5% at the negative loading. In the negative direction, the degradation of load carrying capacity was less than 10% from its peak load even at R=-6.7%. Hysteretic loop was S-shaped with less energy

dissipation with very small residual deformation. Photo 1 shows concrete crushing initiated at R= 1.0%. Compressive yielding of assembling reinforcement (longitudinal reinforcement) occured in both loading direction. The longitudinal reinforcement curtailed at the beam ends carried no tensile force but compressive force and it resulted in compressive yielding. It is suggested to include the compressive yielding of mild steel reinforcement for computing flexural capacity with a higher accuracy. Yielding of strands did not happen and this was confirmed from strain gages placed at the critical section of the beam in this experiment.

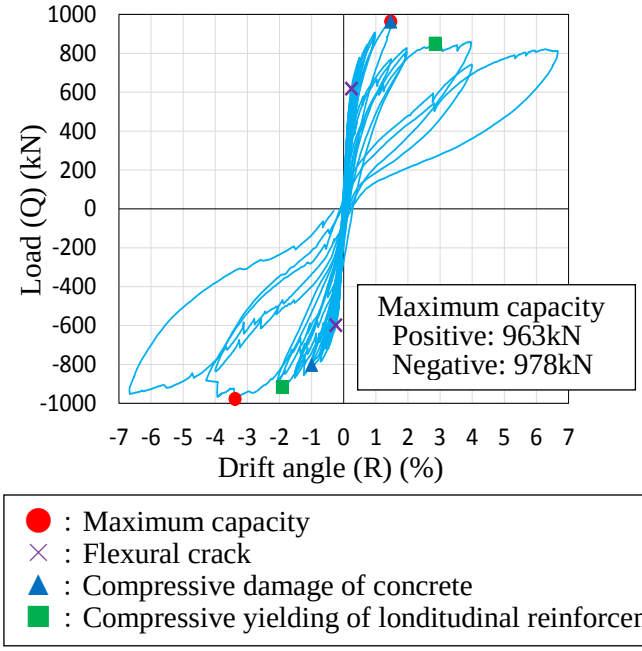

Fig. 3 – Load (Q) – Drift angle (R) relation

(a) Bottom face of beam in north side (b) Side face of (a)

Photo 1 Compressive damage of concrete (R=1.0%)

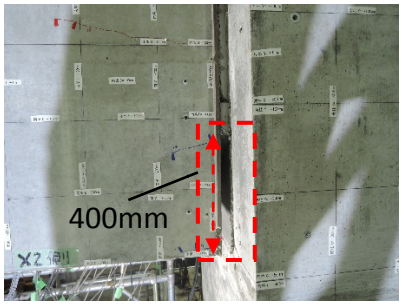

Photo 2 Joint mortar spalling at the South end (R=2.0%)

3.2 Crack patterns

Figure 4 shows the crack patterns at R=2.0%. The spacing of grid lines is 200mm. Blue and red lines show cracks in positive and negative loading directions, respectively. The initial flexure cracks occurred at the bottom part, however no flexural cracks appeared at the upper part due to vertical load. There was no flexural crack near the mortar beam-column interface and the widest cracks (longitudinal cracks) appeared due to compression. RC columns had no cracks until the end of the experiment.

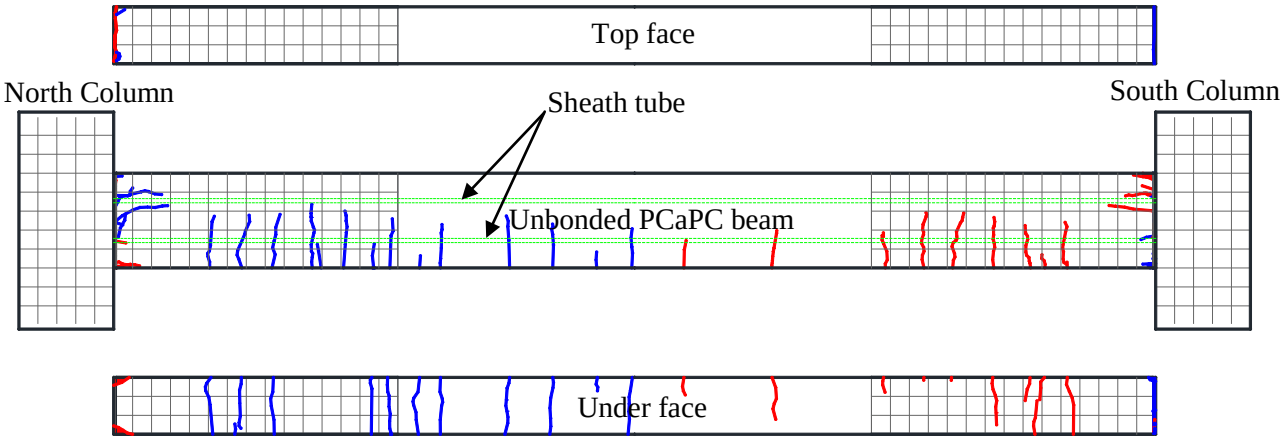

Fig. 4 – Crack patterns (R=2.0%)

3.3 Residual deformation ratio

Figure 5 shows residual deformation ratio, R_{Er} – drift angle of beam, R_b relation. It also shows together with the experimental results of two half-scale cantilever beams (PCa11 and PCa12) and the value of AIJ guidelines formula. The residual deformation ratio is the ratio of the residual displacement to the corresponding peak displacement at the second cycle of loading. Index r in Eq. (3) is the residual drift angle listed in the AIJ guidelines for bonded cantilever PC beams with width of 150mm, depth of 300mm and shear span ratio of 6.0. Index R_{Er} is calculated by dividing r with the peak drift angle, R_b.

$$r = \frac{0.3 \cdot (1.1 - \lambda_t)(R_p \times 100)^{\frac{3+\lambda_t}{2}}}{100} \tag{3}$$

R_p : the corresponding peak drift angle, λ_t : prestressing ratio and $\lambda_t = \frac{T_{py}}{T_{py} + T_y}$

T_{py} : yield force of tendons (kN), T_y : yielding tensile force of longitudinal reinforcement (kN), given as T_y=0 here.

PCa20 shows similar trend with PCa11 and PCa12. Considering the fact that R_{Er} exceeds 50% for ordinary reinforced concrete beams for R_b>1%, R_{Er} was very small and demonstrated the excellent low-damage capability of the unbonded post-tensioned precast concrete beams. Residual deformation ratio, R_{Er}, of PCa20, PCa11 and PCa12 were smaller than that of Eq. (3) when R_b was larger than 1.0%.

3.4 Residual crack width

Figure 6 shows the variation of maximum residual crack width up to R_b=2.0%. It also includes the experimental results of two half-scale cantilever beams and the value by the AIJ guidelines as expressed in Eq. (4). Two types of values were used for the residual deformation angle, R_r with the case of using Eq. (3) and experimental values of a full scale specimen, PCa20. Blue and red of solid lines are residual crack width in north side and south side. Dotted lines are experimental results of 1/2 scale test and calculated results of Eq. (4).

$$w_{r,f} = \frac{1}{n_f} \cdot \alpha \cdot (D - x_n) \cdot R_r \tag{4}$$

$w_{r,f}$: residual flexural crack width (mm), n_f : equivalent number of flexural cracks, given as 2 here, α : ratio of the flexural deformation over the total deformation of the member, given as 0.95 here, x_n : distance from the extreme compressive fiber of the section to the neutral axis (mm), R_r : residual deformation angle.

The residual flexural crack width of a full-scale beam and two half-scale beams was less than 0.2mm until R_b=2.0%. For serviceability limit state in PC flexural members, the residual crack width is defined less than 0.2mm, so these experimental values indicate high damage controlling ability. However, if longitudinal cracks at the critical area of the beam were considered, the residual crack width was over 0.2mm. This longitudinal cracks were due to compression of prestressing force. In calculated results of Eq. (4), the computed values were good up to R_b=1.0%, but the computed values in the case of using R_r of PCa20 was larger than residual crack width of PCa20 when R_b was larger than 1.0%.

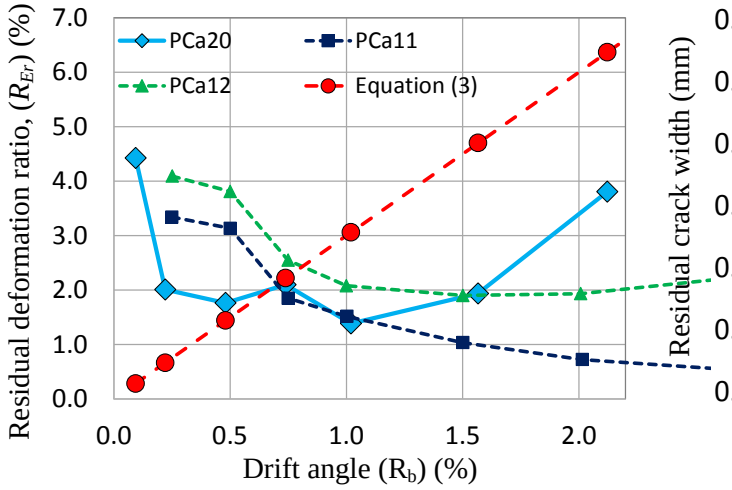

Fig. 5 – Residual displacement ratio (R_{Er})

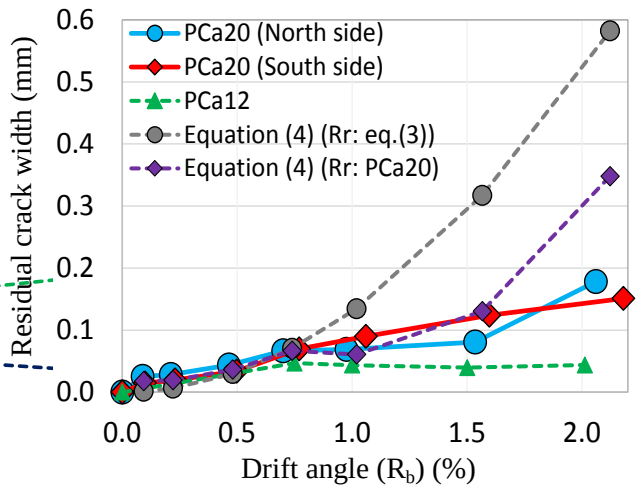

Fig. 6 – Residual crack width

3.5 Equivalent damping ratio

Figure 7 shows variation of equivalent damping ratio, h_{eq}. It also shows experimental results of two half-scale cantilever beams and calculated value by Eq. (5), the AIJ guidelines formula. Equation (5) is for bonded prestressed reinforced concrete cantilever beams. These values including 1/2 scale beams are smaller than that of ordinary reinforced concrete beams, which normally have 10% to 20% for R_b at 2.0%.

$$h_{eq} = \frac{0.9}{\lambda + 0.4}\sqrt{R_p - 0.01} - 2.2\lambda(R_p - 0.01) + 0.05 \qquad (5)$$

R_p : drift angle at peak, λ : prestressing coefficient.

For PCa20 as well as PCa11 and PCa12, h_{eq} was less than 5%. Therefore, in case of using unbonded PCaPC beams as seismic elements, deformation response will be large, so energy dissipation elements need to be added to buildings. Calculated value of h_{eq} by using Eq. (5) was larger than experimental values.

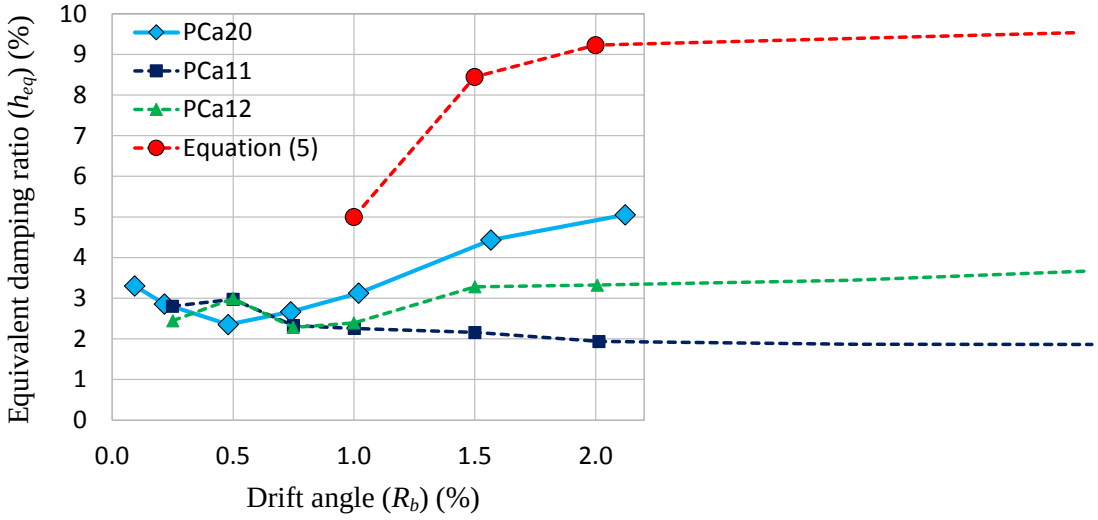

Fig. 7 – Equivalent damping ratio (h_{eq}) – Drift angle of beam, R_b relation

4. Conclusions

An experimental test was conducted on a full-scale unbonded post-tensioned precast concrete H-shaped beam-column assemblage to study seismic behavior and damage levels. The conclusions are summarized.

- The experimental result showed satisfactory seismic performance with minor damage and less residual drift. Residual flexural crack width was less than 0.2mm up to R_b=2.0%. In addition, residual deformation ratio was less than 5%. It indicates that an unbonded post-tensioned precast concrete beam is effective to control the damage and able to achieve quick recovery to maintain the continuity of the building functions after an earthquake.
- Equivalent damping ratio, h_{eq} of the specimen including two half-scale cantilever beams was less than 5% up to R_b=2.0%. This value is very small and seismic response will be large, so energy dissipation elements need to be added to buildings.
- The AIJ guidelines formula for residual displacement ratio and residual crack width were conservative compared to experimental results.

5. Acknowledgements

The research was funded by the Association for Sustainable Building Systems. The authors acknowledge the committee members of the Association for Sustainable Building Systems for valuable comments. The authors also express their special thanks to graduate students at Tokyo Institute of Technology, Prof. Ohmura and his students at Tokyo City University for their help at experimental work. We acknowledge the Materials and Structures Laboratory of Tokyo Institute of Technology for their collaborative research projects (PI: Prof. Kono).

6. References

[1] Priestley, M.J.N. (1991): Overview of the PRESSS Research Program, *PCI Journal*, Precast/Prestressed Concrete Institute, 36(4), pp. 50-57.

[2] Priestley, M.J.N. (1996): The PRESSS Program Current Status and Proposed Plans for Phase III, *PCI Journal*, Precast/Prestressed Concrete Institute, 41(2): pp. 22-40.

[3] Priestley, M.J.N., Sritharan, S., Conley, J.R. and Pampanin, S. (1999): Preliminary Results and Conclusions from the PRESSS Five-Storey Precast Concrete Test-Building, *PCI Journal*, Precast/Prestressed Concrete Institute, 44(6), pp. 42-67.

[4] Englekirk, R.E. (2002): Design-Construction of the Paramount - A 39-story Precast Prestressed Concrete Apartment Building, *PCI Journal*, Precast/Prestressed Concrete Institute, 47(4), 56-71.

[5] Marriott, D., Pampanin, S. and Palermo, A. (2008): Quasi-static and pseudo-dynamic testing of unbonded post-tensioned rocking bridge piers with external replaceable dissipaters, *Earthquake Engineering and Structural Dynamics*, DOI: 10.1002/eqe.857, www.interscience. wiley.com.

[6] Architectural Institute of Japan (2015): Guidelines for Structural Design and Construction of Prestressed Concrete Buildings Based on Performance Evaluation Concept (Draft). (In Japanese)

[7] Moriguchi. et.al (2015): Damage evaluation of precast concrete beams post-tensioned with unbonded tendons, *Summaries of Technical Papers of Annual Meeting*, Architectural Institute of Japan, C2, pp. 733-736. (In Japanese)

[8] Architectural Institute of Japan (2004): Guidelines for performance evaluation of earthquake resistant reinforced concrete buildings. (In Japanese)